

MINIREVIEW OPEN ACCESS

Assessment of Dry Cathode Configuration in Anion Exchange Membrane Water Electrolysis: A Mini Review

Kiran Kiran¹ | Edwin Bumenn¹ | Hans Kungl¹ | Eva Jodat¹ | André Karl¹ | Rüdiger-A. Eichel^{1,2,3}¹Institute of Energy Technologies (IET-1), Fundamental Electrochemistry, Forschungszentrum Jülich, Jülich, Germany | ²Institute of Physical Chemistry, RWTH Aachen University, Aachen, Germany | ³Faculty of Mechanical Engineering, RWTH Aachen University, Aachen, Germany**Correspondence:** Kiran Kiran (k.kiran@fz-juelich.de)**Received:** 24 May 2025 | **Revised:** 30 July 2025 | **Accepted:** 8 August 2025**Funding:** The authors gratefully acknowledge the financial support by the German Federal Ministry of Education and Research (BMBF) within the AEM-Direkt (Grant 03HY130F).**Keywords:** dry cathode anion exchange membrane water electrolysis (AEMWE) | ion exchange capacity | water uptake | water management | operating parameters | electrolyte feed

ABSTRACT

Anion exchange membrane (AEM) electrolysis is one of the most promising water electrolysis technologies, combining the advantages of proton exchange membrane (PEM) electrolysis, such as high gas purity, high current densities and dynamic operation, while using cheap transition metal electrocatalysts known from alkaline water electrolysis (AWE). AEM water electrolysis (AEMWE), when operated liquid (electrolyte or water) free (dry) at the cathode side, offers simplified water management, reducing the balance-of-plant. Numerous factors, such as cell design, membrane properties, flow rate of electrolyte and operation parameters, directly or indirectly, impact the performance of AEMWE, which becomes even more vital when the cathode compartment is operated liquid free. Herein, this work presents a comprehensive overview of several factors involved in the performance of a dry cathode AEMWE. Advancements and challenges in membrane materials, asymmetric electrolyte feeds and operating parameters were analysed. Finally, to have a durable and efficient AEMWE, this article discusses current development on the dry cathode AEMWE technology and outlines prospective avenues for further improving the system.

1 | Introduction

Rising energy consumption and climate change motivate the transition to a renewable energy economy. Hydrogen technologies have the potential to play a significant role in this regard as hydrogen (H₂) can be used both as a fuel and for energy storage. However, currently most of the H₂ is produced via steam methane reforming and coal [1, 2] leading to significant carbon dioxide emissions. Water electrolysis technology has emerged as a viable approach for the H₂ generation as it can be coupled with the intermittently available renewable energy and thus serve as a bridge to sectors such as transportation and heavy industry [3]. Primarily, three types of low-temperature electrolysers are employed for

the H₂ generation: alkaline water electrolysis (AWE), proton exchange membrane water electrolysis (PEMWE) and anion exchange membrane water electrolysis (AEMWE) [4–6]. The classic AWE electrolysers employ highly alkaline electrolyte and non-noble transition metal catalysts coated electrodes that are separated by a diaphragm. However, the low current density and gas crossover leading to a low gas purity in classic AWE are often reported as main issues in the literature [7, 8]. PEMWE uses a PEM conducting protons (H⁺) from the anode to the cathode, allowing cell operation at comparatively high current densities. However, the use of acidic environment leads to inevitable use of noble metals as electrocatalysts, thereby increasing the capital cost [6, 9, 10]. On the contrary, AEMWE operates in an alkaline

This is an open access article under the terms of the [Creative Commons Attribution](https://creativecommons.org/licenses/by/4.0/) License, which permits use, distribution and reproduction in any medium, provided the original work is properly cited.

© 2025 The Author(s). *Electrochemical Science Advances* published by Wiley-VCH GmbH.

environment with the AEM conducting anions (OH^-) aiming to combine the advantages of AWE and PEMWE. As it operates in an alkaline environment, non-noble electrocatalysts can be used, alleviating the cost of system [11, 12].

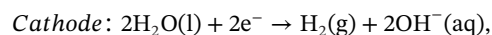
Essentially, two types of feed configurations are possible in AEM electrolyzers. In one configuration, typically both the cathode and the anode are supplied with electrolyte or water also known as wet configuration, whereas in the dry cathode configuration, only the anode side is supplied with electrolyte or water. Another configuration which could be of interest is dry anode configuration, where anode compartment is kept liquid free; however, it is seldom employed [13–15]. At a commercial scale, ‘Hystar’ is employing a dry anode configuration in PEMWE [16, 17]. Each of the configurations has its advantages and limitations, respectively. In the case of a liquid-fed anode and cathode, generally better ionic conductivity can be achieved. The risk of the membrane electrode assembly (MEA) drying out can be eliminated due to a continuous supply of electrolyte, ensuring sufficient reactant (OH^- and H_2O) is available for the reaction [18, 19]. However, the risk of electrolyte crossover, water management and degradation due to the corrosive alkaline environment can make this configuration complex to handle [20]. On the contrary, when the cathode is kept liquid free (dry cathode configuration), it can provide advantages over the issues mentioned above. This setup is being utilized on a commercial scale by ‘Enapter’ who integrated it into their large-scale hydrogen production processes [21]. In addition, a dry cathode configuration has the potential to provide hydrogen with a higher purity since complex liquid–gas separation setup is not necessarily required at the outlet of cathode when compared to a configuration with a liquid feed on both the anode and the cathode. However, the challenges of a dry cathode configuration include the lack of hydration leading to drying out of the membrane, lower ion conductivity and potential degradation issues at higher current densities [22]. Recently, some investigations have been done on the dry cathode concept in AEMWE; however, the literature regarding the same is very limited.

Studies have investigated the influence of several parameters, highlighting the effect of the binder amount [23], the membrane type and its thickness [24], the water distribution, the used electrocatalyst [25] and the catalyst loading [26]. However, despite the focused research, a comprehensive overview elucidating the complex interplay between these parameters in a dry cathode configuration in AEMWE is still missing. The purpose of this study is to bridge the gap among various particularities of the dry cathode concept in order to provide a more holistic picture. This perspective will provide an overview covering different factors affecting cell performance of AEMWE operated in a dry cathode configuration.

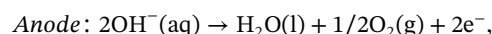
2 | AEMWE Configurations: Mechanistic Understanding

In principle, two different cell configurations have been studied in the literature in AEMWE. In the wet configuration, an alkaline electrolyte solution or de-ionized water (DIW) is supplied to both the cathode and the anode. In most of the research studies, potassium hydroxide (KOH) is employed as a supporting

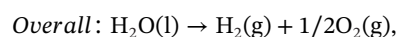
electrolyte instead of DIW due to its higher ion conductivity [8] and the stability of the non-noble materials [27]. Nickel, often used material in AEMWE, however, gets unstable at anode side under acidic or near-neutral pH (~ 9) making alkaline medium beneficial for its durability [28]. The AEM conducting hydroxide ions is inserted between the cathode and the anode. When bias is applied to the AEMWE, water dissociates into OH^- and produces H_2 gas at the cathode via the hydrogen evolution reaction (HER). The OH^- ions are transported from the cathode to the anode via the AEM due to the applied electric field (Figure 1a). These OH^- ions then produce water and O_2 at the anode via the oxygen evolution reaction (OER) [8, 26]. The two half-cell reactions and the overall reaction can be written as follows:



$$E^\circ = -0.83 \text{ V versus SHE}$$



$$E^\circ = 0.40 \text{ V versus SHE}$$



$$E^\circ = 1.23 \text{ V versus SHE}$$

where E^0 refers to the reversible potential and SHE stands for the standard hydrogen electrode. In the alkaline environment, two water molecules are required at the cathode to produce H_2 . Thus, the water transport from the anode to the cathode plays a crucial role in determining the overall performance [26].

On the other hand, in the case of a dry cathode configuration (i.e., single-side feed mode), the anode is purged with liquid and the cathode is kept liquid free (Figure 1b). Water is transferred to the cathode by diffusion due to the concentration gradient, which might cause K^+ ions to diffuse as well [29]. OH^- ions move from the cathode to the anode, and the water at the cathode is also dragged to the anode in the hydration shell of OH^- ions via an electro-osmotic drag. As the only source of hydration at the cathode is by water diffusion from the anode to the cathode, the generated H_2 stream separation can be achieved with a small liquid–gas separator. However, it may lead to the drying out of the cathode due to insufficient hydration.

At higher current densities, conventional systems are susceptible to a number of issues owing to several factors such as higher reaction rates and an imbalance in water distribution. With increasing current density, the hydrogen and oxygen production rates increase, leading to a higher consumption of water in electrochemical reaction. The inadequate water stoichiometry ratio might lead to dehydration in the anode compartment or cause local drying out [30]. This effect appears more prominent in the case of a dry cathode configuration [29]. Another potential issue in the conventional system could be the increase in gas evolution in both compartments which may lead to formation of large number of gas bubbles. This, in turn, may lead to the surface coverage of catalyst by gas bubbles, which consequently affects the overall performance [5, 26, 31]. This effect may be less evident at the cathode side in the case of dry cathode configuration.

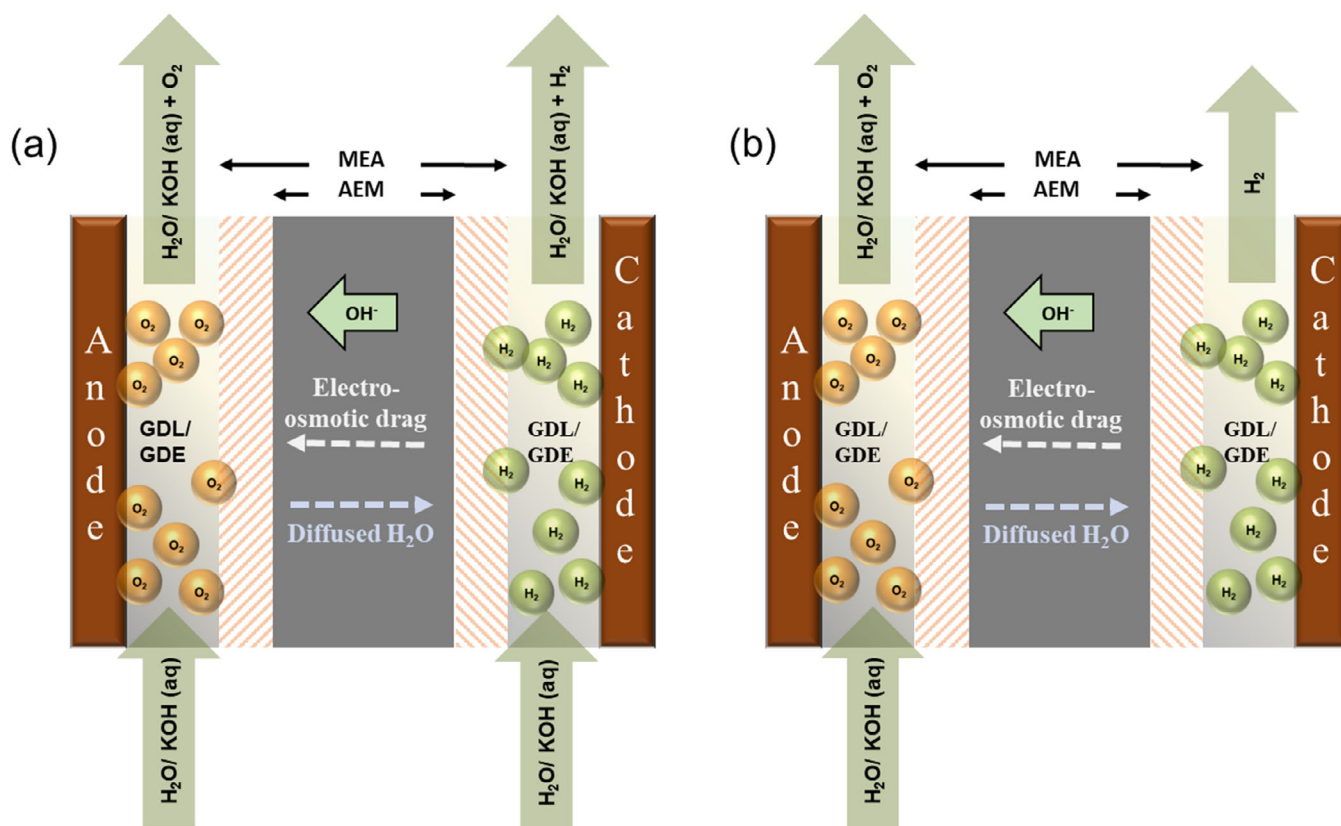


FIGURE 1 | Schematic of AEMWE in (a) wet configuration and (b) dry cathode configuration. AEM, anion exchange membrane; GDL, gas diffusion layer; MEA, membrane electrode assembly.

Gas crossover can also be an issue, typically more pronounced in the case of AWE where a diaphragm is employed to separate both compartments. However, gas crossover is also a potential issue in membrane electrolyzers (AEMWE and PEMWE) since the membrane is not perfectly impermeable. Principally, both oxygen and hydrogen can permeate through the membrane. However, hydrogen crossover is more commonly observed owing to its small molecular size, leading to higher diffusion [32]. The hydrogen crossover to the anode side can lower the overall efficiency of the process and can pose safety concerns due to potential buildup of an explosive gas mixture (>4% of H_2 in O_2) [26]. However, a threshold of 2% is generally kept to mitigate safety risks [33]. Several factors, for instance, operating current density, pressure, temperature and membrane thickness, can affect the H_2 crossover [26].

In 2025, a report by Witte et al. highlighted the influence of contact pressure on H_2 crossover in conventional AEMWE [34]. The increase in contact pressure (0.5–2.5 MPa) led to higher gas contamination (H_2 in O_2 content) from 1.4 to 2.9 vol% respectively at a current density of 0.1 A cm^{-2} [34]. To mitigate gas crossover, either thicker membranes can be used or the microstructure of the membrane can be modified [26]. It is important to note that thick membranes typically lead to higher resistances comprising the cell performance. Moreover, H_2 crossover was reduced by 56% by adding 2% zirconia to a Sustainion membrane [35]. H_2 crossover is also a critical issue in dry cathode configurations, possibly even more so due to the higher concentration gradient of H_2 across the AEM as the liquid is not present to act as

an additional barrier for evolved gas [36]. In addition, electro-osmotic drag may facilitate transport of the dissolved hydrogen in the water molecules to the anode side. It can further contribute to the crossover, although this effect is likely to be less prominent in the case of dry cathode configuration. The topic of H_2 crossover in specifically dry cathode setup remains largely unexplored, with only very few experimental investigations to date [37].

One of the key performance indicators in water electrolysis is the ‘polarization curve’ for evaluating the cell performance by providing insights into the current-voltage behaviour and thus highlighting the losses associated with different electrolyser components and parameters. Figure 2 represents the schematic of losses involved in electrolytic performance influencing the shape of the polarization curve of an AEMWE. During the cell operation, practical voltage is perpetually higher than the reversible voltage (E^0) owing to the different loss mechanisms in the electrolytic system. Characteristically, these voltage losses can be subdivided into three different types of losses. Activation losses comprise the losses due to the cathode and the anode kinetics and are more evident at low current densities [38]. These losses still persist at higher current densities; however, they are not as significant compared to the ohmic losses. The linear region at mid-section of current densities is attributed to the ohmic losses. These ohmic losses are mainly attributed to anion transfer through the membrane and partly to the resistances of other cell components. Additionally, the electrode surface coverage due to the generated gas bubbles may indirectly contribute to the ohmic losses as well. This particular effect becomes even

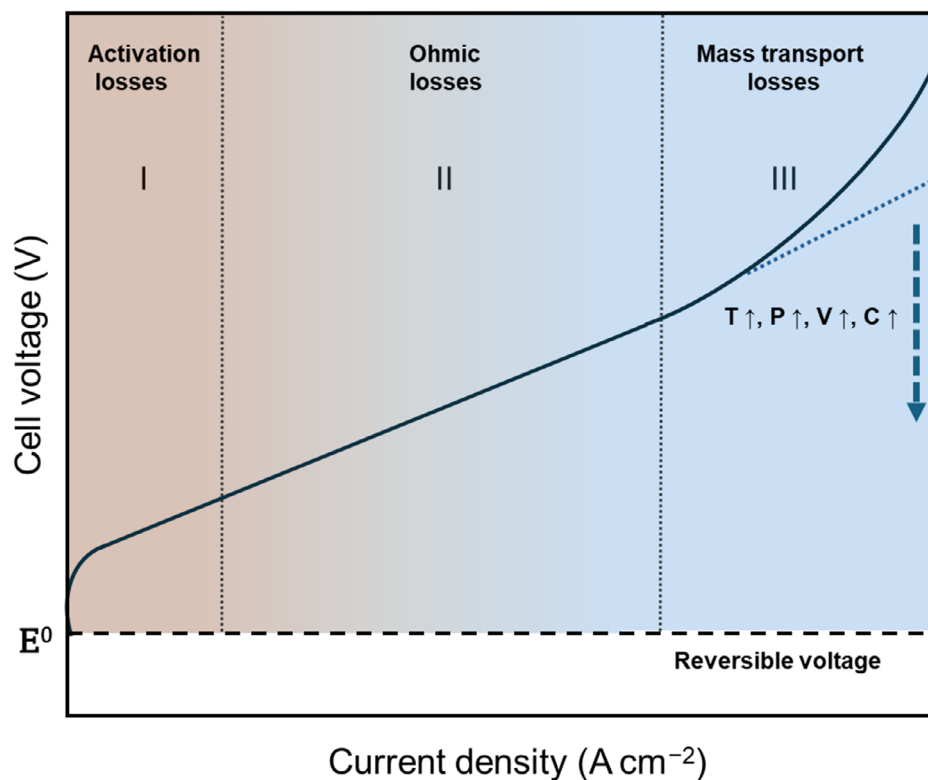


FIGURE 2 | Schematic of the distribution of losses at various sections of a typical polarization curve of an AEMWE. This can be influenced by several different operating parameters such as temperature, cell compression, flow rate and concentration of electrolyte. As these operating parameters change, the cell voltage can change accordingly due to their influence on different processes involved in AEMWE. Source: Adapted from Ref. [38].

more pronounced at higher current densities, highlighted by the steep increase in the voltage (mass transfer losses; see third section in Figure 2). Moreover, insufficient electrolyte supply (low reactant) may cause starvation at higher current densities, contributing to the mass transfer losses, especially in a dry cathode configuration. Under these conditions, the conductivity of the membrane will also reduce, leading to steady increase in ohmic losses, compounding to the mass transfer losses. Several operating parameters (temperature, flow rate, electrolyte concentration, cell compression, H₂ backpressure and others) can affect all these losses, influencing the shape of the polarization curve (Figure 2).

Besides the hydration issue, one also needs to consider other variables such as the electrolyte feed and other operating conditions. Figure 3 depicts the classification of the factors affecting cell performance specifically in a dry cathode setup. In this setup, cell performance is influenced by two different types of parameters categorised as the operational and the material parameters. Operational parameters are the ones which directly influence the performance and are subdivided into operating conditions such as electrolyte feed, current density, flow rate, temperature and relative humidity. Conversely, the indirect factors such as the ion exchange capacity (IEC) of the ionomer used itself or as an AEM and its amount constitute the material parameters.

3 | Ionomer Effect

AEMs are the fundamental core component of AEMWE technology. An ideal AEM should be highly conductive for the OH⁻ ions,

be mechanically and thermally robust, have optimal water uptake (WU) and be chemically stable [39, 40]. Generally, AEMs are constituted by a polymer backbone with cationic groups which are responsible for conferring anionic selectivity and conductivity [41]. The capability of anion transport by an ionomer used in AEM depends greatly on the water retention, also known as the WU. Although Donnan exclusion typically prevents KOH permeation, some retention may still occur in ion-solvating membranes or at elevated KOH concentrations (≥ 1 M) [42], which is undesirable. The physical quantity which influences the water retention is the IEC of a membrane [29]. Hence, IEC plays a pivotal role in a dry cathode configuration, especially as water management is a key factor for long-term operation at a higher current density. In principle, IEC represents the number of exchangeable ions for the respective membrane per unit weight and is expressed in meq g⁻¹ or mmol g⁻¹ [43]. Different methods, such as titration, spectroscopy (i.e., UV-Vis) and ion-selective methods, can be used to measure the IEC of H⁺ or OH⁻ [44, 45]. WU, on the other hand, is the measure of the mass changes when exposed to water [45]. The WU can be defined as

$$\text{WU} = \frac{(m_w - m_d)}{m_d} \times 100 \%$$

where m_w is mass of the wet membrane, and m_d is mass of the dry membrane, respectively.

As optimal water management is vital in a dry cathode setup, understanding the link among IEC, WU and the cell voltage is even more important [45].

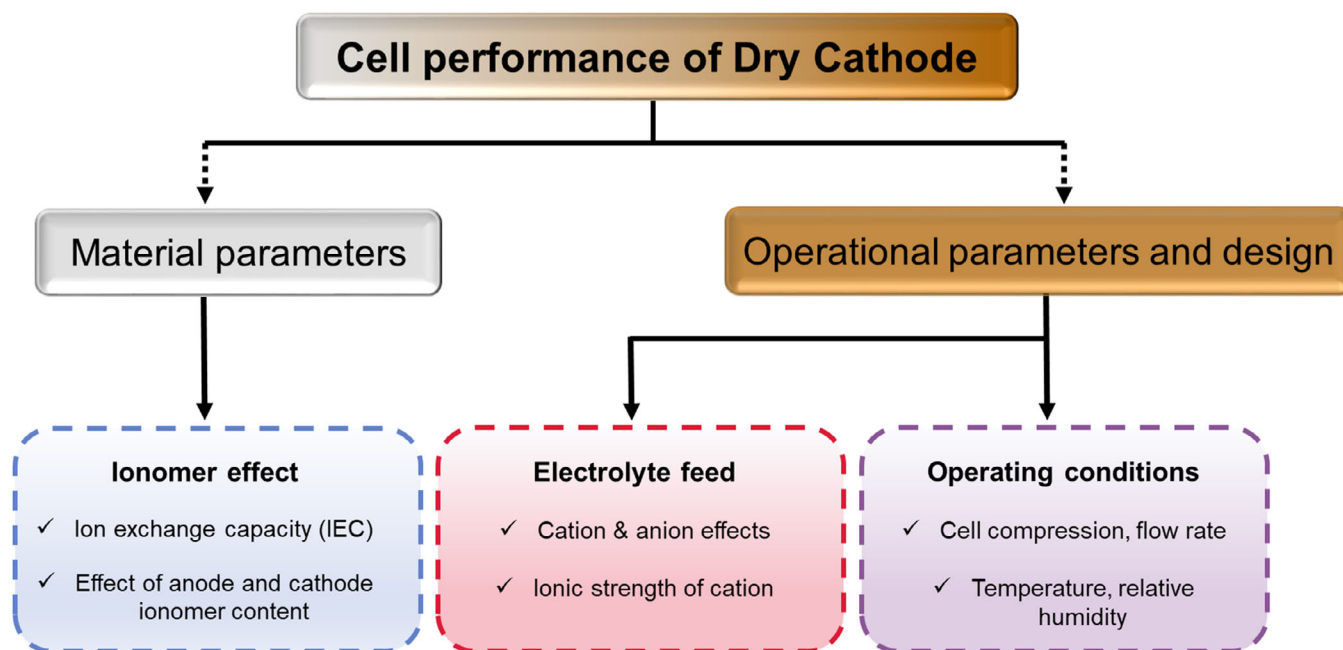


FIGURE 3 | Schematic of factors affecting the cell performance of dry cathode configuration are divided into three categories.

The molecular structure of an AEM consists of a primary functional group and a polymer backbone. Traditionally, quaternary ammonium groups are used as functional groups with a polymer backbone such as polystyrene, polysulphone, poly(ether sulphone) or poly(phenylene oxide) via benzylic methylene group [41, 46]. The molecular structure of other AEMs demonstrates the use of an imidazolium cationic group and a metal (ruthenium)-based cationic group as well. The use of different functional groups offers their own advantages and limitations, respectively. Quaternary ammonium groups show high hydroxide ion conductivities, whereas imidazolium functional groups attached to the polymer backbone exhibit improved chemical stability. Most of the state-of-art commercial membranes employ quaternary ammonium groups. Only a few commercial membranes use imidazolium cationic group such as Aemion and Sustainion AEM [47].

Figure 4 (hollow triangle and solid sphere symbols, respectively) depicts the influence of IEC on the WU and cell voltage of commercial and lab-tested membranes. All the sample's initials are referenced next to the symbols presented in Figure 4. For commercial membranes (Figure 4, red symbols), the average IEC is presented for simplicity. Some of the studies express IEC as meq g^{-1} , whereas the others present it in mmol g^{-1} . However, both of the units are the same provided the net charge or the valency on the structure is unit [48]. Important to note is that these commercial membranes are generally used in AEMWE where both the catholyte and the anolyte are fed to the cathode and the anode, respectively (Table 1).

Because the dry cathode configuration depends on the water diffusing from the anode, there is a great need for ionomer or membrane with varying IEC and WU. Chen et al. developed four ionomers based on piperidinium, that is, poly(fluorenyl-co-biphenyl piperidinium-14) (PFBP-14), poly(fluorenyl-co-terphenyl piperidinium-8) (PFTP-8), PFTP-13

and crosslinked x-PFTP, in which three PFTP-based ionomers were used to synthesize AEMs [6]. For comparison, these three PFTP ionomer-based AEMs are presented in Figure 4 as lab-tested ionomer-based membranes (Figure 4, grey symbols) [6]. Among these three PFTP-based membranes, PFTP-13-based membrane exhibited a WU of up to 73% with IEC of 2.80 mmol g^{-1} (Figure 4, grey triangle). A commercial PTFE-reinforced Sustainion (X37-50 grade T) AEM exhibited a relatively lower WU (36%) under similar conditions (Figure 4, red triangle). However, the values of WU for commercial and lab-tested ionomer-based membranes do not exhibit a clear trend over the entire range of IEC values. The cell voltages of both commercial and lab-tested ones are compared at a constant current density of 1 A cm^{-2} and 60°C (Figure 4, red and grey spheres, respectively). The lab-tested membranes showed a slightly lower cell voltage than the commercial membranes. However, there does not appear to be noticeable trend in the cell voltages [6]. All the details of the referenced samples in Figure 4 have been presented in a tabular form (Table 1).

Given the discrepancies in conditions across studies, drawing comparisons proves difficult. Compounding this, there is little to no literature available that systematically studies the correlation of IEC, WU and the cell voltage in the dry cathode configuration. An important aspect is the amount of ionomer used at the cathode and anode side. Cathode ionomer contents between 10% and 40% were tested, with a 25% cathode ionomer content exhibiting superior performance, reaching 2 V at a current density of 3.5 A cm^{-2} with the AEMWE operating at 60°C [6].

An investigation by Cho et al. focused on the effect of the PTFE polymer content at the anode varying between 5 and 20 wt% [23]. In the case of a low binder content (5 and 9 wt%), initially a higher current density at a constant voltage of 1.8 V was observed, in contrast to the other two binder content samples showing lower performances initially. However, the trend for the higher and

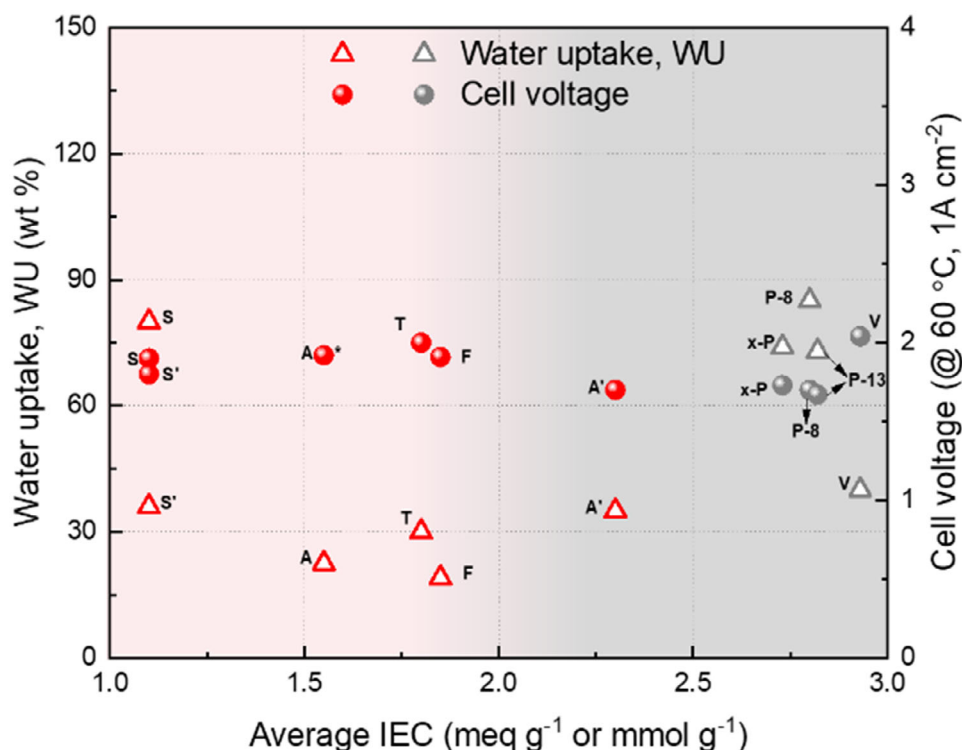


FIGURE 4 | Ion exchange capacity (IEC) of commercial and in-house built membranes plotted versus water uptake (WU) and cell voltage at a current density of 1 A cm^{-2} [6, 18, 20, 24, 50–54]. Cell voltage (A^*) is presented at 50°C . Red symbols represent commercial samples, and grey symbols represent lab-tested samples.

TABLE 1 | Data of the samples for ion exchange capacity (IEC), water uptake (WU) and cell voltage shown in Figure 4.

Label	Sample	Average IEC, meq g^{-1} or mmol g^{-1} [Ref.]	WU, wt% [Ref.]	Cell voltage @ $60^\circ\text{C } 1 \text{ A cm}^{-2}$, V [Ref.]	Catalyst (anode, cathode)	Flow configuration
S'	PTFE-reinforced Sustainion AEMs X37-50 grade T	1.1 [24]	36 [6]	1.8 [6]	IrO_2 , Pt/C	Dry cathode
T	Tokuyama A201	1.8 [20]	30 [20]	2.0 [49]	CuCoO_x , $\text{Ni}/(\text{CeO}_2\text{-}$ $\text{La}_2\text{O}_3)/\text{C}$	Dry cathode
x-P	x-PFTP (AEM)	2.73 [6]	74 [6]	1.73 [6]	IrO_2 , Pt/C	Dry cathode
P-8	PFTP-8 (ionomer and AEMs)	2.8 [6]	85 [6]	1.7 [6]	IrO_2 , Pt/C	Dry cathode
P-13	PFTP-13 (AEM)	2.82 [6]	73 [6]	1.67 [6]	IrO_2 , Pt/C	Dry cathode
S	Sustainion X37-50	1.1 [24]	80 [24]	1.9 [18]	NiFe_2O_4 , NiFeCo	Dual-side
F	Fumatech FAA3-3-50	1.85 [50]	19 [50]	1.91 [51]	IrO_2 , Pt/C	Dual-side
A'	Aemion AF1-HNN8-50-X	2.3 [52]	35 [52]	1.7 [53]	Ir black, Pt/C	Dual-side
A	Aemion AF1-HNN5-50-X	1.55 [52]	22.5 [52]	1.92 [53]	Ir black, Pt/C	Dual-side
V	V-2-H-1	2.93 [54]	40 [54]	2.04 [54]	NiFe_2O_4 , NiFeCo	No info

Note: 1 M KOH was used as the electrolyte in all of the studies mentioned in the table. Dual-side in the flow configuration refers to liquid flowing in both the anode and the cathode.

Abbreviation: AEM, anion exchange membrane.

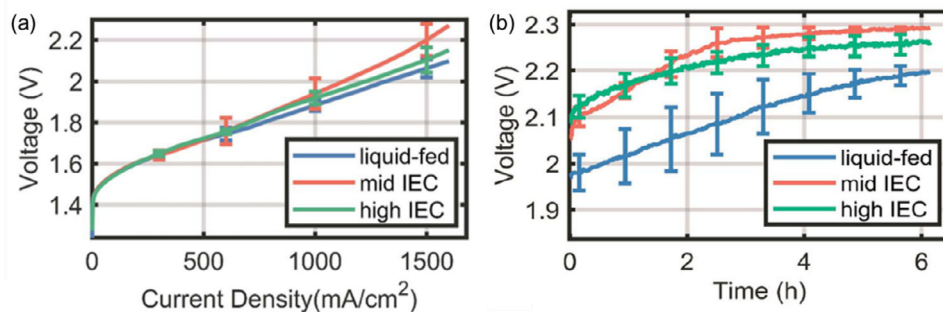


FIGURE 5 | (a) Polarization curve for three different systems with a liquid-fed cathode and dry cathode operation with either a mid or high IEC polymer used in the cathode layer; (b) degradation test done at operating temperature of 60°C and constant current density of 1 A cm⁻². [29] 0.1 M KOH was used as the electrolyte. IEC, ion exchange capacity. *Source:* (a) and (b) Reproduced with permissions from RSC Advances under the licence <https://creativecommons.org/licenses/by/3.0/>.

lower PTFE content samples reversed with increased time [23]. With a higher binder content of 20 wt%, a current density of 1.07 A cm⁻² at 1.8 V was measured after 1300 cycles compared to the lower binder content of 5 and 9 wt%, reaching <0.4 and <0.6 A cm⁻², respectively. This increased performance with a higher anode binder content was correlated to less catalyst loss and an optimized pore structure leading to better mass transport and kinetics [23].

A subsequent study examined the water distribution for mid (1.8–2.2 meq g⁻¹) and high IEC (2.3–2.6 meq g⁻¹) samples at elevated current densities [29]. Neutron imaging was conducted in order to experimentally observe the water distribution [29]. Indeed, an imbalance in the water distribution in the MEA exists in a dry cathode configuration. This trend becomes even more pronounced at elevated current densities (>0.6 A cm⁻²) evident from the polarization curve (Figure 5a).

The KOH-fed (0.1 M) cathode exhibited lower cell voltages at higher current densities compared (>0.6 A cm⁻²) to the dry cathode operation with mid and high IEC owing to the better membrane humidification [29]. Furthermore, degradation test was performed at a constant current density of 1 A cm⁻² for a time duration of 6 h (Figure 5b). Comparing the cell performances of all three configurations, the authors observed higher degradation rate for initial 2 h in dry cathode operation, especially in case of mid IEC with a degradation rate of 75 mV h⁻¹ to a degradation rate of 45 mV h⁻¹ for high IEC and KOH-fed cathode. Overall, KOH-fed cathode achieved a better performance compared to the other configurations [29]. The overall performance of AEMWE is greatly affected by chemical stability of the membrane in alkaline environment [55]. The nucleophilic nature of OH⁻ can lead to either scission of polymer backbone or attack the functional group reducing the IEC and the mechanical stability of AEM as well. The primary degradation paths affecting the functional groups include nucleophilic substitution (SN₂), Hoffman elimination or formation of ylide intermediate in conventional systems, induced by OH⁻ attack [42, 56, 57]. In the dry cathode configuration, the availability of free OH⁻ is significantly reduced compared to the conventional system. Though OH⁻ can still be produced locally during water electrolysis, its limited concentration might suppress degradation pathways that rely on nucleophilic attack such as SN₂ and Hoffmann; however, they may still occur with a limited prevalence. Furthermore,

mechanisms such as radical oxidative species-induced degradation may also be observed due to the generation of reactive oxygen species [57]. The degradation mechanisms of AEMs with different functional groups and polymeric backbones in the conventional system have been discussed in detail in several reviews [42, 45, 56, 58]. However, no experimental study is available discussing possible degradation mechanisms in the dry cathode configurations specifically which makes it challenging to understand membrane/ionomer degradation. Future work encompassing analytical techniques, such as Fourier-transform infrared spectroscopy (FTIR) and nuclear magnetic resonance (NMR), is required to deconvolute degradation mechanism of the AEM, particularly in dry cathode configuration. Additionally, the correlation of IEC on WU and cell voltages should be systematically studied.

4 | Electrolyte Feed Effect

The impact of the electrolyte feed on the performance and stability of AEMWE is significant as it controls the pH near the electrode–electrolyte interface. The appropriate control of the concentration of the supporting electrolyte is critical for maintaining the ionic conductivity. Typically, aqueous potassium hydroxide (KOH) in the range between 1 and 10 wt% is fed to the cell, thereby ensuring an efficient water splitting reaction. Different types of electrolytes feeding (i.e., single or dual-side, asymmetric feed) are reported in the literature [15]. Leng et al. studied scenarios of the cell testing at 50°C with different feed (DIW) modes [59]. The MEA was fabricated with catalyst coated substrate (CCS) method, with an aminated Radel poly(sulphone) as the applied ionomer. A stable cell voltage of 2.25 V at a current density of 0.2 A cm⁻² (for more than 500 h was achieved when DIW was circulated through both the anode and the cathode [59]. In another case, where DIW was only fed to the anode side, cell voltage increased rapidly at the initial stage of electrolysis; however, it became more stable afterwards yielding around 300 h of stable operation. On the contrary, when DIW was fed to the cathode only, relatively large degradation rates were observed, resulting in a stable operation of up to 196 h [59]. Interestingly, the stability of the system was extended up to 500 h of operation, when the cathode was fed for the initial 2 h of the operation and the anode feed was employed for the rest of the testing time [59]. These findings indicate that sufficient

hydration to the cathode compartment, especially in the initial period of operation, is crucial for efficient and durable operation. The effect of the supporting electrolyte feed was investigated by distinction between an 'initial' and an 'operating' feed [23]. The 'initial feed' can be considered as a form of conditioning with a supply of either DIW or KOH for 10 min. The 'operating feed' on the other hand describes the electrolyte feed during electrolysis operation [23]. It was shown that supplying KOH as the 'initial feed' results in better early performance and long-term operation, especially when operated in a dry cathode configuration. This better performance was attributed to an improvement in mass transport [23].

As high pH electrolytes (i.e., pH \sim 14) are generally chosen as the electrolyte owing to their better ionic conductivity, they also pose several disadvantages, such as a corrosive environment and the shunt current issues during operation [60]. One alternative could be to use neutral pH media or DIW; however, the ionic conductivity of such media is typically lower, leading to the ohmic losses. A study illustrated the systematic investigation of the impact of metal salts when added to near-neutral pH media on AEMWE [60]. Sodium perchlorate was used as the baseline salt and was compared to the DIW. Addition of NaClO₄ (10 mM) to the anolyte improved the performance markedly and yielded an operating voltage of 2.58 V at a current density of 0.5 A cm⁻² compared to an operating voltage of 2.77 V with DIW [60]. The effects of two different salts (KNO₃, NaHCO₃) were compared to the baseline NaClO₄ salt as well, with KNO₃ showing the best performance. Employing a saline anolyte compared to pure water leads to a reduced ohmic resistance, resulting in a smaller operating voltage. Ion crossover was minimized owing to the combined effect of the membrane charge and the electric field direction in the dry cathode configuration [60]. Some other studies also probed the use of different electrolyte feed such as pure water and potassium bicarbonate [61, 62].

An important parameter in the dry cathode AEMWE operation is so-called cation and anion effects. A recent study unveiled the effect of alkali metal cations (i.e., Li⁺, Na⁺, K⁺ and Cs⁺) combined with the anolytes containing low hydroxide concentrations [63]. With the change in size of the cation, the cathode overpotential varied, whereas the overpotential at the anode side was unchanged as the hydroxide concentration present in the anolyte remained same. Sodium hydroxide (NaOH, 0.01 M) was used as the anolyte and nitrate salts with varying alkali metal cations (LiNO₃, NaNO₃, KNO₃, CsNO₃, 0.15 M) were experimentally measured [63]. In the study at hand, the anode overpotential was lowest when the anolyte contained only NaOH. However, when nitrate salts were added, anode overpotentials increased slightly. This could be attributed to the availability of more nitrate ions in the ionomer covering some of the catalyst, leading to a low hydroxide concentration in the ionomer [63].

On the contrary, cathode overpotential was affected majorly by the addition of nitrate salts in the anolyte. Among all the four cations, K⁺ exhibited the smallest cathode overpotential at high current densities and showed the overall best performance in the order from K⁺ < Na⁺ < Li⁺ < \sim Cs⁺ [63]. This trend in performance was correlated with the dynamic ionic radius and the cation mobility. As the AEM is not perfectly rejecting salts, cations can diffuse and migrate through AEM and are attached to

the hydration shell. Among all the four cations, Li⁺ had a small ionic radius and a large hydration shell (Figure 6), resulting in an overall larger dynamic ionic radius impeding its mobility [63]. Contrary to this, K⁺, which shows the best performance, reaching a cell potential of 1.802 V at 1 A cm⁻², exhibits the smallest dynamic ionic radius (Figure 6). In addition to this finding, a long-term stability of 1000 h of operation at 1 A cm⁻² at 60°C with the anolyte containing K⁺ ions (0.01 M KOH + 0.15 M KNO₃) was reported [63]. Given the results in Figure 6, Na⁺ also can be an interesting alternative to K⁺ ions as it has good hydration capacity and good mobility, especially in dry cathode configuration at even higher current densities of 2 A cm⁻² or more. Kiessling et al. studied the influence of the catholyte supporting electrolyte on the AEMWE performance while applying 1 M KOH as the anolyte flow [64]. They noted a favourable effect at the higher current densities owing to the lower high frequency resistance (HFR) while using DIW or KOH at the cathode. The alteration of anions from OH⁻ to CO₃²⁻ or NO₃⁻ degraded overall cell performance, attributable to the increased HFR and anion poisoning at the HER side [64].

Different feed modes appear to be influencing the long-term operation of AEMWE systems. The system's durability shows improvement when KOH is supplied during the initial phase of operation. Furthermore, performance variations may arise due to added cations and anions in the electrolyte, necessitating further research.

5 | Operating Parameters and Design

5.1 | Operating Parameters

Operating parameters mainly consist of cell compression, operating temperatures, pressure, flow rates and different conditioning procedures and so forth [27]. A work in 2021 highlighted the effect of cell compression on overall performance of the AEMWE [65]. The authors examined the influence of mechanical compression on the MEA by varying cathode gas diffusion layer (GDL) thickness and number of gaskets used in the cell. A set of commercial Toray papers (T30, T60, T90 and T120) were tested with different thickness, keeping all the other parameters (i.e., fibre diameter, density and porosity) constant [65]. With an increase in cell compression, cell performance was shown to improve, with T120 performing the best. The reason behind the improved performance was attributed to a better interfacial contact leading to a lower contact resistance [65]. However, in this work, both cathode and anode were supplied with DIW as the electrolyte.

The variable which directly influences the kinetic rate constants, thermodynamics and ionic conductivity is the operating temperature. At a constant overpotential of 591 mV, varying operating temperatures from 50°C to 90°C led to an increase in the cell performance [66]. The performance improved from 0.5 to 0.7 A cm⁻² corresponding to 50°C and 90°C, respectively. For each 10°C change, an increment of \sim 0.05 A cm⁻² in the current density was reported using Fumasep FAA-3-PK-75 (Fumatech). This increase in the current density was attributed to the better ionic conductivity and catalytic activity at higher temperatures [66]. Similar observations were made using a Fumasep FAA3-50

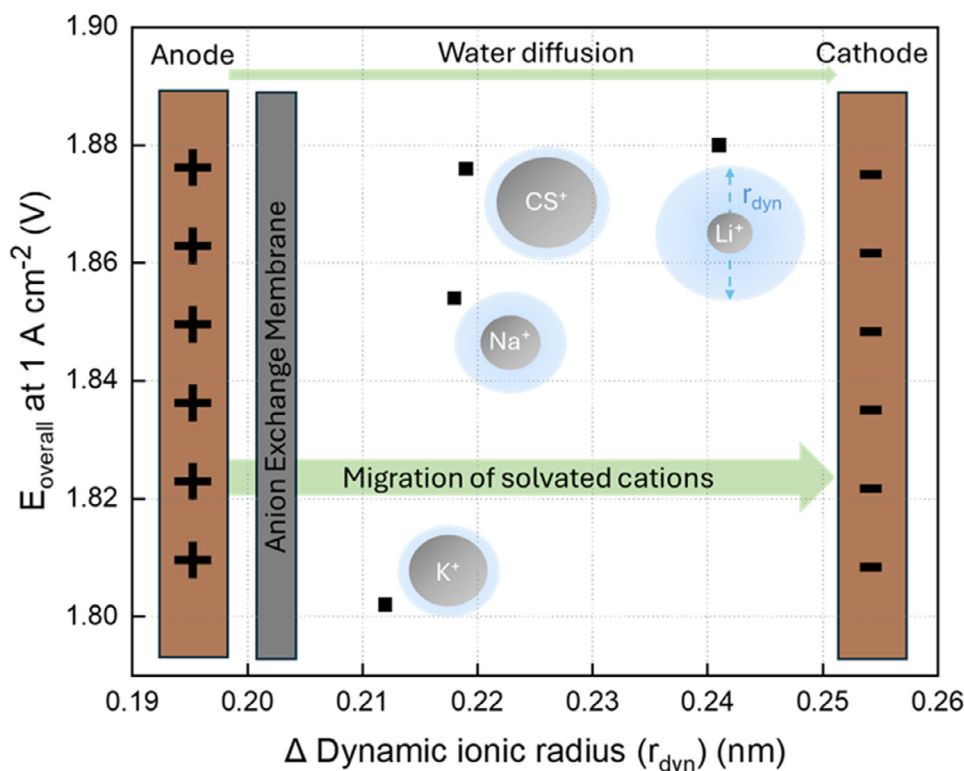


FIGURE 6 | Schematic of overall voltage at 1 A cm^{-2} as a function of dynamic ionic radius of Li^+ , Na^+ , K^+ and Cs^+ . Source: Adapted from Ref. [63].

(Fumatech) membrane with a NiFe_2O_4 anode and a Pt/C cathode in the temperature range from 30°C to 60°C [67]. At a constant voltage of 2.2 V , an increase of 0.5 A cm^{-2} per 10°C temperature gradient was reported. A maximum of 3 A cm^{-2} was achieved at 60°C , attributed to a lowered ohmic and kinetic resistance, thus resulting in a better ionic conductivity and kinetics [67]. From the above-discussed results, there is a trend observable in that the cell performance improves with increasing operating temperatures; however, it is hard to compare these specific results because the two studies employed different membranes and systems.

The effect of anolyte concentration, operating temperature (30 – 60°C) and flow rate (1 – 9 mL min^{-1}) on the AEMWE performance was further investigated by Azam et al. [68] Anolyte concentration was varied from 0.5 to 2 M KOH at an operating temperature of 30°C and a flow rate of 6 mL min^{-1} [68]. Polarization curves revealed a cell voltage of 2.48 V at 1.2 A cm^{-2} for 2 M KOH compared to a cell voltage of 2.62 V for 0.5 M KOH . These performance changes indicate that with a higher concentration of KOH , a better ionic conductivity across the membrane can be reached. Thus, the cell voltage was reduced, in turn, reaching a voltage efficiency of $\sim 60\%$ (Figure 7a) at 1.2 A cm^{-2} . Comparing polarization curves at different temperatures revealed an inverse relationship between the cell voltage and the temperature increase [68]. Cell voltage decreases with an increase in the temperature, reaching $\sim 2.39 \text{ V}$ and a voltage efficiency of $\sim 62\%$ (Figure 7b) at 1.2 A cm^{-2} for 60°C . This impact of temperature was attributed to an increase in mobility of the OH^- ions at higher temperatures, thus increasing the availability of OH^- ions at the catalyst surface for reactions to occur [68]. At lower temperatures, the mobility of the OH^- ions becomes slower due to a lower diffusion constant, causing increase in ohmic resistance.

Furthermore, lower temperature can slow down the reaction kinetics, contributing to a higher charge transfer resistance [68]. However, the flow rate of the electrolyte showed minimal effect on the cell performance evidenced from Figure 7c. Increasing the flow rate from 1 to 9 mL min^{-1} improves the mass transfer and decreases the cell resistance. A cell voltage of $\sim 2.469 \text{ V}$ was obtained at a current density of 1.2 A cm^{-2} (active area of 5 cm^2) and flow rate of 9 mL min^{-1} , whereas a cell voltage of $\sim 2.499 \text{ V}$ was measured at 1 mL min^{-1} . Despite the minimal impact of the flow rate on the cell performance, its influence is still critical since it pertains to the active area. According to EU harmonised protocol, $2 \text{ mL min}^{-1} \text{ cm}^{-2}$ is established as a recommended standard [69].

Discrepancies in system components and configurations across studies make it challenging to directly compare the influence of the flow rates reported in the literature. Moreover, the choice of flow rates often seems to be random without a systematic basis. As the O_2 and H_2 bubbles are formed at the anode and cathode, respectively, it is important to remove the bubbles from catalyst surface to avoid blocking active sites. Higher flow rates may help in removing the bubbles faster and might help avoid the membrane dehydration, specifically in a dry cathode configuration. However, one must be careful as the higher flow rate can also potentially enhance degradation of the electrode [68]. According to observations from literature, the operating temperature and the electrolyte concentration proved to be significantly affecting the cell performance, whereas only a minor effect was observed for the flow rate.

Applying backpressure of H_2 at the cathode side is another interesting factor as it can lower the need of downstream processing, cutting down the H_2 separation and compression cost [27, 70]. Ito

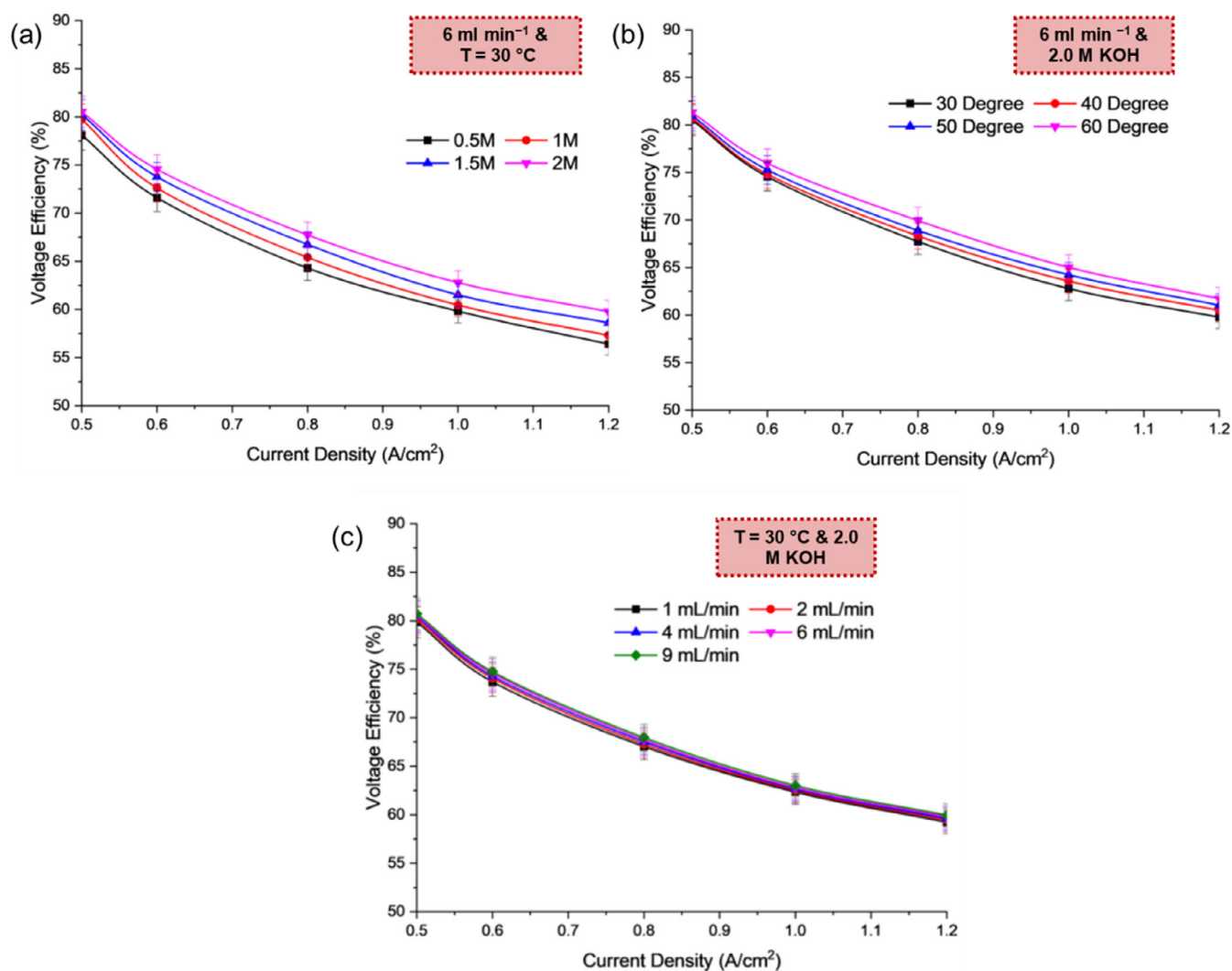


FIGURE 7 | Voltage efficiency versus current density (a) with varying concentration of KOH (0.5 to 2 M); (b) with varying operating temperature (30–60°C); (c) with different flow rates of electrolyte (1–9 mL min⁻¹) [68]. Voltage efficiency was defined as the ratio of the thermo-neutral voltage to the cell voltage in percentage. *Source:* (a)-(c) Reproduced with permission from polymers under the licence <https://creativecommons.org/licenses/by/4.0/>.

et al. in 2019 demonstrated the effect of H₂ backpressure in the cathode compartment [37]. A systematic performance analysis (cell voltage, resistance, H₂ content in anode compartment and dew point of produced H₂) of a cell at three different cathode backpressures (1, 5 and 8.5 bar) was carried out. CuCoO_x was used as the anode catalyst, Pt/C was used as the cathode catalyst, and A201 (Tokuyama) membrane was employed for the OH⁻ transport [37]. A minimal effect of H₂ backpressure on the cell overpotential was reported and indicated that the pressure range might not be sufficient for determining a trend. Interestingly, the obtained dew point in outstream H₂, which, in turn, indicates the relative humidity, decreases with increasing backpressure. It may be beneficial in terms of the reducing downstream cost for post processing; however, it may also lead to the membrane dehydration, especially when the cathode is operated liquid free [37]. Furthermore, H₂ crossover (H₂ in O₂) was increased with an increase in cathode backpressure and at lower current density (0.1 A cm⁻²). A maximum value of 4 vol% of H₂ in O₂ at 8.5 bar and 0.1 A cm⁻² was observed that is higher than explosion limit. Thus, attention should be paid while operating in this operation range.

H₂ crossover was found to decrease with increase in the current density (0.2 to 1 A cm⁻²) for all the cathode backpressures [37].

Procedures, such as pre-treatment or conditioning protocols, are widely discussed for PEMWE [71]; however, for AEMWE, such protocols are not widely implemented yet. Pre-treatment or conditioning refers to the process of preparing the electrolysis system components (i.e., membrane or MEA) to achieve optimal performance, durability and efficiency of the process. It may include the activation of the membrane or MEA, break-in procedure at a constant current or potential (static mode) and dynamic operation. Studies in the past report the activation of membrane by dipping it in alkaline solution (0.5 to 3 M KOH) for several hours up to 1 day extending up to several days either ex situ or in situ [23, 66]. Alternatively, accelerated stress testing in the forward and reverse direction may also govern the AEMWE performance. Although operational variables are critical in determining AEMWE efficacy, there is limited research on systematic evaluation of these parameters, especially in a dry cathode design.

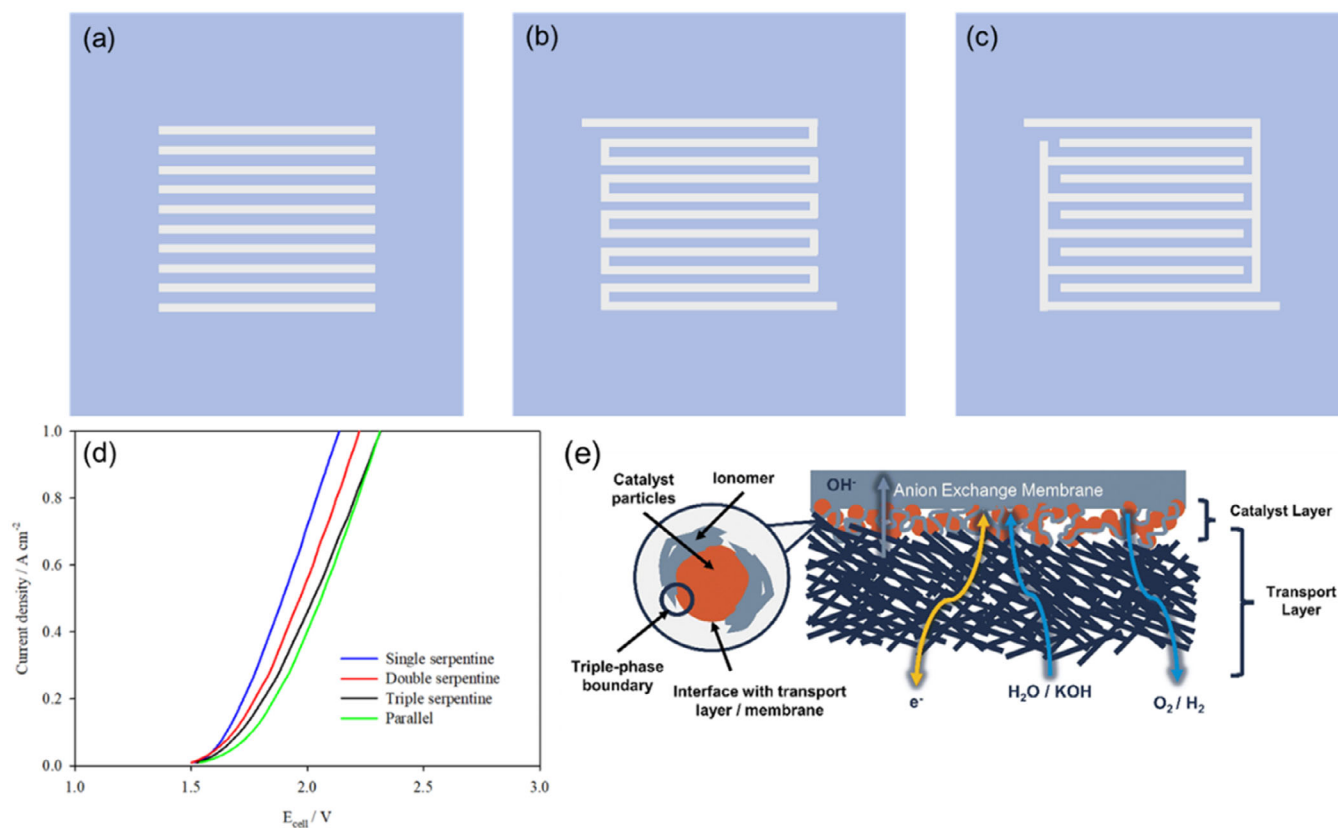


FIGURE 8 | Schematic of flow fields (a) parallel; (b) serpentine; (c) interdigitated and (d) polarization curve comparing the performance of different flow fields in the conventional setup; (e) schematic of PTL depicting the movement of $\text{H}_2\text{O}/\text{KOH}$ showing triple phase boundary. *Source:* (d) Reproduced with permission [75] <https://creativecommons.org/licenses/by/4.0/>; (e) reproduced with permission [27] <https://creativecommons.org/licenses/by-nc/3.0/>.

5.2 | Cell Design

Despite recent progress in AEMWE [69, 72], it still needs more in-depth understanding and standardization in terms of cell architecture and operating parameters, especially for dry cathode configurations. For the cell architecture, this may include material choices for bipolar plates (BPP), porous transport layers (PTL) and different electrode compositions. The BPP serves various purposes such as the current distribution and managing the fluid (reactant and product) distribution across the electrolyser components, accounting about 40% of the stack cost [39]. Considering the conditions in an AEMWE, generally graphite is used as the BPP for the cathode side. Besides graphite, other metals such as stainless steel (SS), nickel (Ni) and titanium (Ti) (anode) BPP have also been employed [51, 73, 74]. Although the choice of cheaper materials can lower the stack cost, these materials can also passivate and corrode, compromising the efficacy of the system in the longer run. The flow fields are particularly important in water electrolysis because there is two-phase flow constituting of liquid flow and gas bubbles. The main function of the flow fields includes uniform water distribution to the catalyst layer (CL), gas removal produced at the cathode or the anode and minimizing the pressure drop. Flow fields can be used separately as well as integrated with the BPP. Typically, different flow field designs exist such as parallel, serpentine and interdigitated (Figure 8a–c). The difference between parallel and serpentine flow fields is generally the way liquid flows through the channel. In the case of

parallel flow field, the liquid flows through the electrode surface in the same direction via all flow channels. In serpentine flow fields, on the contrary, the liquid flows through continuous zigzag path. However, there is no general agreement regarding which of these geometries provides the best performance.

Four flow field designs (parallel, single serpentine, double serpentine and triple serpentine) with the dimensions of 2 mm width and 3 mm depth were examined in a 10 cm^2 cell [75]. Polarization curves (Figure 8d) were recorded in 1 M KOH at 333 K with a flow rate of 270 mL min^{-1} . The results demonstrate that the cell with a parallel flow field exhibited a higher cell voltage in the entire current range compared to the serpentine flow fields. This performance difference could be due to the nonuniform flow, temperature and pressure distribution in the parallel flow channels [75]. Notably, with the triple serpentine design, cell voltages are higher compared to the single serpentine flow field, especially at higher current densities (Figure 8d). It was arguably due to a lower mass flow rate of the electrolyte in each of the three channels because the electrolyte flow is distributed across channels. In other words, higher mass flow rate of electrolyte in the case of single serpentine flow channel allows efficient reactant utilization and product removal compared to the double and triple serpentine. Thus, it resulted into relatively lower cell voltage, leading to better cell performance [75]. It is important to point out that this study employed conventional system (dual-side feed). Currently, the efforts related to influence of flow field

designs, especially for the dry cathode AEMWE, are scant in the literature. Systematic investigation of flow field designs (parallel, serpentine, interdigitated and mesh/grid) at the cathode should be conducted so that it can facilitate gas removal and manage the pressure and generated heat.

The PTL generally is present next to the either side of the AEM or MEA. The transport layer facilitates gas diffusion, homogeneous current distribution and water transport and provides mechanical support (i.e., fibre, foam or woven network) to the CL (Figure 8e) [26]. Typically, carbon or Ni-based materials are used as the PTL or GDL on the cathode side, and Ti PTL (either only Ti or platinumized Pt-Ti) is used on the anode side because the oxidizing environment can lead to enhanced degradation of the PTL [51]. For instance, Park et al. studied the performance of nickel-iron oxyhydroxide (NiFeOOH) for an AEMWE system [76]. Spray coated Pt/C (40 wt%) on Fumasep FAA-3-50 was used as the cathode layer, whereas NiFeOOH-PTL electrodeposited onto a PTL via a CCS approach was employed as the anode catalyst. The Ni_{0.56}Fe_{0.44}OOH exhibited the best performance among the studied compositions, yielding a current density of ~3.6 A cm⁻² at a cell voltage of ~1.9 V [76]. Furthermore, the number of gaskets seemed to have an effect on the cell performance because it also alters the thickness and hence the cell compression [65]. The system with one gasket (cathode) along with an SS (SS10) GDL exhibited an improvement of 0.11 V, yielding a cell voltage of 2.13 V at 0.5 A cm⁻². However, one needs to be careful with the number of gaskets utilized, because higher compression can lead to increased H₂ crossover from the cathode to the anode [65]. A comparative study was conducted on three different PTLs (SS-PTL, Pt-Ti and Ni) for anodes in AEMWEs [57]. The SS-PTL exhibited the highest electroactivity towards the OER, with the lowest charge transfer resistance. A cell voltage of 2 V was achieved at 4 A cm⁻² demonstrating best device performance. Furthermore, the SS-PTL electrode was compared with conventional (iridium oxide, IrO_x and cobalt oxide, Co₃O₄) CLs coated on a Pt-Ti PTL [57]. Until a current density of 1 A cm⁻², IrO_x exhibited the best performance; however, the cell voltage increased up to 2.2 V compared to the SS-PTL with ~2 V at 4 A cm⁻². This performance variation was attributed to the instability of the catalyst caused by high amount of gas and heat generation in the conventional CL especially at higher reaction rates [57]. Considering these functionalities, it is crucial to tune the BPP, PTL and flow field for the optimal electrolyser operation. In the case of dry cathode operation, the water management will additionally be crucial for optimizing performance, especially when scaling up this configuration.

Additional factors impacting performance entail the architectural components such as the type of catalyst, the amount of loading and the material choice of electrolyser cell or stack components. The microstructure (e.g., porosity) of CL is vital as the direction of water transport is via the membrane in the dry cathode configuration compared to conventional wet AEMWE [15]. Thus, the interplay between ionomer and CL is even more indispensable here. A study highlighted the water distribution across the AEM in electrolytic cells with single or double membranes. In addition, they studied the influence of porosity of the cathode CL by means of two different methods: ultrasonic stirring (less porous cathode CL) and high-speed thin film mixing (highly porous cathode CL) [77]. They showed less gradient in the water distribution or more

water at cathode side in the cell with low porosity cathode CL, both in single- and double-membrane configurations, compared to high porosity cathode CL. Furthermore, the polarization curves showed better performance when single membrane was used owing to the Ni low resistance and concentration overpotential [77]. Several articles and comprehensive reviews are available for detailed discussion on the catalyst loading and stack components [5, 15, 26, 65].

6 | Conclusion and Perspective

In summary, operating AEMWE in dry cathode configuration can be advantageous in several aspects, offering better and simplified water management and allowing the use of a non-corrosive environment, thereby reducing the capital cost and making it more cost-effective. The influence of different parameters such as material (ionomer or AEM), operational (temperature, flow rate and electrolyte feed) and cell design (flow field pattern) affect the cell performance of the dry cathode AEMWE. Although the developments in this field have shown a great potential alternative for AEMWE cell design, there is still a significant lack of data for a dry cathode operation of AEMWEs. On the basis of the existing literature work, we suggest several steps to remedy this.

As electrolyte or water is supplied to the cathode by diffusion through the AEM, it is vital to optimize the IEC and WU. The IEC should not be too low as the WU will be lower, causing dry out. On the contrary, a higher IEC will lead to a higher WU, thereby causing swelling of the membrane, which might also be detrimental [78, 79]. In order to tune the IEC, different ionomers should be used at the cathode and anode, respectively. More hydrophobic ionomers may be used at the anode side, as this side is continuously being fed by water or electrolyte, and hydrophilic ionomers can be employed at the cathode side, as more hydration is required here, especially at higher reaction rates [63, 78, 80]. The initial feed is important for the conditioning, as it will influence the durability and performance of the cell. There is no optimized protocol available for the conditioning of dry cathode electrolysers yet. The existing literature on the effect of the flow rate affecting cell performance is limited and mostly related to the traditional AEMWE (dual-side feed). Studies have reported different electrolyte flow rates; however, there is a lack of in-depth investigation, particularly in the context of cell configuration. Comprehensive screening is essential to assess the effect of flow rate, particularly in the wide range (10–50 mL min⁻¹) which is especially important when there is no electrolyte at the cathode side. This assessment is critical because it ensures transport of the OH⁻ ions through the membrane to the cathode side for the reaction to occur and to avoid membrane dehydration. An approach to prevent membrane dehydration could be to use either higher electrolyte concentration on the anolyte side [68] or to supply some amount of electrolyte at cathode side in vaporized form [64], primarily at current densities beyond >0.6 A cm⁻². However, there is a trade-off between better hydration and system components degradation at higher KOH concentrations which should be considered as well.

Furthermore, higher temperatures exhibited a favourable effect on the cell performance; however, higher temperatures can also

accelerate degradation and compromise durability of the system. Ex situ and in situ diagnostics are needed to understand degradation mechanisms in more depth. Because higher temperatures will lead to a change in the dew point, it will consequently change the relative humidity across the AEM. It is necessary to systematically study the effect of humidity on the AEM or the full MEA to deconvolute ion transport by means of in situ electrochemical impedance spectroscopy (EIS) [81]. The application of neutron imaging (ex situ and in situ) has been demonstrated to be an effective method for mapping hydration gradients across the AEM/MEA [29]. Furthermore, small-angle x-ray scattering (SAXS) can be useful in understanding the microstructure and hydrophilic/hydrophobic domains of AEM or MEA [82, 83]. To comprehend the chemical degradation mechanisms occurring in the membrane, it is imperative to employ techniques such as FTIR and NMR [57]. These methodologies have been demonstrated to be highly effective and should be utilized in conjunction with one another to ensure comprehensive analysis. In order to effectively monitor the gas crossover, it is essential to incorporate specialized sensors into the system. In addition, gas chromatography (GC) measurements should be conducted to obtain comprehensive data on the gas composition in the anodic compartment [37]. The existing literature on AEMWE employs broadly two different classes of catalysts: PGM-based catalysts and non-PGM-based catalysts. Due to these two concurrent types of catalysts, it is better to benchmark them separately.

Although the merits and utility of the dry cathode AEMWE are promising, there are still many unanswered domains which need to be addressed. Moreover, it is crucial to have a more standardized and optimized protocol. Going forward, addressing the aforementioned challenges may lead to advancing dry cathode AEM technology; however, it requires thorough and critical investigation approaches.

Acknowledgements

The authors gratefully acknowledge the financial support by the German Federal Ministry of Education and Research (BMBF) within the AEM-Direkt (grant number 03HY130F).

Open access funding enabled and organized by Projekt DEAL.

Conflicts of Interest

The authors declare no conflicts of interest.

Data Availability Statement

Data sharing is not applicable to this article as no datasets were generated or analysed during the current study.

References

1. D. Das and T. Veziroglu, "Advances in Biological Hydrogen Production Processes," *International Journal of Hydrogen Energy* 33, no. 21 (2008): 6046–6057.
2. K. Zhang, X. Liang, L. Wang, et al., "Status and Perspectives of Key Materials for PEM Electrolyzer," *Nano Research Energy* 1 (2022): e9120032.
3. M. Kraglund, M. Carmob, G. Schiller, et al., "Ion-Solvating Membranes as a New Approach Towards High Rate Alkaline Electrolyzers," *Energy & Environmental Science* 12, no. 11 (2019): 3313–3318.

4. M. Mandal, "Recent Advancement on Anion Exchange Membranes for Fuel Cell and Water Electrolysis," *ChemElectroChem* 8, no. 1 (2021): 36–45.
5. D. Li, A. R. Motz, C. Bae, et al., "Durability of Anion Exchange Membrane Water Electrolyzers," *Energy & Environmental Science* 14, no. 6 (2021): 3393–3419.
6. N. Chen, S. Y. Paek, J. Y. Lee, J. H. Park, S. Y. Lee, and Y. M. Lee, "High-Performance Anion Exchange Membrane Water Electrolyzers With a Current Density of 7.68 A cm⁻² and a Durability of 1000 Hours," *Energy & Environmental Science* 14, no. 12 (2021): 6338–6348.
7. P. Haug, M. Koj, and T. Turek, "Influence of Process Conditions On Gas Purity in Alkaline Water Electrolysis," *International Journal of Hydrogen Energy* 42, no. 15 (2017): 9406–9418.
8. J. Liu, Z. Kang, D. Li, et al., "Elucidating the Role of Hydroxide Electrolyte on Anion-Exchange-Membrane Water Electrolyzer Performance," *Journal of the Electrochemical Society* 168 (2021): 054522.
9. U. Babic, M. Suermann, F. N. Büchi, L. Gubler, and T. J. Schmidt, "Critical Review—Identifying Critical Gaps for Polymer Electrolyte Water Electrolysis Development," *Journal of the Electrochemical Society* 164, no. 4 (2017): F387.
10. O. Schmidt, A. Gambhir, I. Staffell, A. Hawkes, J. Nelson, and S. Few, "Future Cost and Performance of Water Electrolysis: An Expert Elicitation Study," *International Journal of Hydrogen Energy* 42, no. 52 (2017): 30470–30492.
11. C. C. Pavel, F. Cecconi, C. Emiliani, et al., "Highly Efficient Platinum Group Metal Free Based Membrane-Electrode Assembly for Anion Exchange Membrane Water Electrolysis," *Angewandte Chemie (International ed in English)* 53 (2014): 1378–1381.
12. X. Tang, L. Xiao, C. Yang, J. Lu, and L. Zhuang, "Noble Fabrication of Ni–Mo Cathode for Alkaline Water Electrolysis and Alkaline Polymer Electrolyte Water Electrolysis," *International Journal of Hydrogen Energy* 39, no. 7 (2014): 3055–3060.
13. S. H. Ahn, S. J. Yoo, H. Kim, et al., "Anion Exchange Membrane Water Electrolyzer With an Ultra-Low Loading of Pt-Decorated Ni Electrocatalyst," *Applied Catalysis B: Environmental* 180 (2016): 674–679.
14. S. H. Ahn, B. Lee, I. Choi, et al., "Development of a Membrane Electrode Assembly for Alkaline Water Electrolysis by Direct Electrodeposition of Nickel on Carbon Papers," *Applied Catalysis B: Environmental* 154–155 (2014): 197–205.
15. A. W. Tricker, J. K. Lee, J. R. Shin, N. Danilovic, A. Z. Weber, and X. Peng, "Design and Operating Principles for High-Performing Anion Exchange Membrane Water Electrolyzers," *Journal of Power Sources* 567 (2023): 232967.
16. B. Espedal Kindem, M. Fredriksen, and J. Jaschke, "Control-Oriented Modeling of Proton Exchange Membrane Water Electrolyzer," Accessed on August 24, 2024 <https://ntnuopen.ntnu.no/ntnu-xmlui/handle/11250/3156461?show=full>.
17. *Hystar*, Accessed on August 25, 2024, <https://hystar.com/leading-the-charge-on-pem-technology/>.
18. Z. Liu, S. D. Sajjad, Y. Gao, H. Yang, J. J. Kaczur, and R. I. Masel, "The Effect of Membrane on an Alkaline Water Electrolyzer," *International Journal of Hydrogen Energy* 42, no. 50 (2017): 29661–29665.
19. M. Đurovič, J. Hnát, C. I. Bernäcker, et al., "Nanocrystalline Fe₆₀Co₂₀Si₁₀B₁₀ as a Cathode Catalyst for Alkaline Water Electrolysis: Impact of Surface Activation," *Electrochimica Acta* 306 (2019): 688–697.
20. C. C. Pavel, F. Cecconi, C. Emiliani, et al., "Highly Efficient Platinum Group Metal Free Based Membrane-Electrode Assembly for Anion Exchange Membrane Water Electrolysis," *Angewandte Chemie International Edition* 53, no. 5 (2014): 1378–1381.
21. Enapter, EUROPEAN PATENT, Accessed on August 27, 2024, <https://patents.google.com/patent/EP2451992B1/en>.

22. J. C. Fornaciari, M. R. Gerhardt, J. Zhou, et al., "The Role of Water in Vapor-Fed Proton-Exchange-Membrane Electrolysis," *Journal of the Electrochemical Society* 167, no. 10 (2020): 104508.
23. M. K. Cho, H. Park, H. J. Lee, et al., "Alkaline Anion Exchange Membrane Water Electrolysis: Effects of Electrolyte Feed Method and Electrode Binder Content," *Journal of Power Sources* 382 (2018): 22–29.
24. G. Lindquist, S. Z. Oener, R. Krivina, et al., "Performance and Durability of Pure-Water-Fed Anion Exchange Membrane Electrolyzers Using Baseline Materials and Operation," *ACS Applied Materials & Interfaces* 13, no. 44 (2021): 51917–51924.
25. M. David, C. Ocampo-Martínez, and R. Sánchez-Peña, "Advances in Alkaline Water Electrolyzers: A Review," *Journal of Energy Storage* 23 (2019): 392–403.
26. N. Du, C. Roy, R. Peach, M. Turnbull, S. Thiele, and C. Bock, "Anion-Exchange Membrane Water Electrolyzers," *Chemical Reviews* 122, no. 13 (2022): 11830–11895.
27. E. K. Volk, M. E. Kreider, S. Kwon, and S. M. Alia, "Recent Progress in Understanding the Catalyst Layer in Anion Exchange Membrane Electrolyzers—Durability, Utilization, and Integration," *EES Catalysis* 2, no. 1 (2024): 109–137.
28. L. Huang, M. J. Hutchison, R. J. Santucci, J. R. Scully, and J. M. Rondinelli, "Improved Electrochemical Phase Diagrams From Theory and Experiment: The Ni–Water System and Its Complex Compounds," *Journal of Physical Chemistry C* 121, no. 18 (2017): 9782–9789.
29. S. Koch, J. Disch, S. K. Kilian, et al., "Water Management in Anion-Exchange Membrane Water Electrolyzers Under Dry Cathode Operation," *RSC Advances* 12, no. 32 (2022): 20778–20784.
30. S. Sun, Y. Xiao, D. Liang, et al., "Behaviors of a Proton Exchange Membrane Electrolyzer Under Water Starvation," *RSC Advances* 5, no. 19 (2015): 14506–14513.
31. F. Arbabi, A. Kalantarian, R. Abouatallah, R. Wang, J. Wallace, and A. Bazylak, "Feasibility Study of Using Microfluidic Platforms for Visualizing Bubble Flows in Electrolyzer Gas Diffusion Layers," *Journal of Power Sources* 258 (2014): 142–149.
32. G. Wijaya, K. Im, and S. Nam, "Advancements in Commercial Anion Exchange Membranes: A Review of Membrane Properties in Water Electrolysis Applications," *Desalination and Water Treatment* 320 (2024): 100605.
33. A. Klinger, O. Strobl, H. Michaels, et al., "Transport of Hydrogen Through Anion Exchange Membranes in Water Electrolysis," *Advanced Materials Interfaces* 12, no. 5 (2025): 2400515.
34. J. Witte, P. Trinke, B. Bensmann, M. Becker, R. Hanke-Rauschenbach, and T. Turek, "Influence of Contact Pressure on Hydrogen Crossover and Polarization Behavior in AEM Water Electrolysis," *Journal of the Electrochemical Society* 172, no. 1 (2025): 014502.
35. B. Motealleh, Z. Liu, R. I. Masel, J. P. Scully, Z. Richard Ni, and L. Meroueh, "Next-Generation Anion Exchange Membrane Water Electrolyzers Operating for Commercially Relevant Lifetimes," *International Journal of Hydrogen Energy* 46, no. 5 (2021): 3379–3386.
36. L. Titheridge and A. Marshall, "The Rationale for a Standardized Testing Protocol for Anion Exchange Membrane Water Electrolyzers," *ACS Energy Letters* 9, no. 3 (2024): 1288–1294.
37. H. Ito, N. Kawaguchi, S. Someya, and T. Munakata, "Pressurized Operation of Anion Exchange Membrane Water Electrolysis," *Electrochimica Acta* 297 (2019): 188–196.
38. H. Lv, J. Chen, W. Zhou, X. Shen, and C. Zhang, "Mechanism Analyses and Optimization Strategies for Performance Improvement in Low-Temperature Water Electrolysis Systems via the Perspective of Mass Transfer: A Review," *Renewable and Sustainable Energy Reviews* 183 (2023): 113394.
39. Q. Xu, L. Zhang, J. Zhang, et al., "Anion Exchange Membrane Water Electrolyzer: Electrode Design, Lab-Scaled Testing System and Performance Evaluation," *EnergyChem* 4, no. 5 (2022): 100087.
40. M. A. Vandiver, B. R. Caire, J. R. Carver, et al., "Mechanical Characterization of Anion Exchange Membranes by Extensional Rheology Under Controlled Hydration," *Journal of the Electrochemical Society* 161, no. 10 (2014): H677.
41. H. Miller, K. Bouzek, J. Hnat, et al., "Green Hydrogen From Anion Exchange Membrane Water Electrolysis: A Review of Recent Developments in Critical Materials and Operating Conditions," *Sustainable Energy & Fuels* 4, no. 5 (2020): 2114–2133.
42. D. Henkensmeier, W. Cho, P. Jannasch, et al., "Separators and Membranes for Advanced Alkaline Water Electrolysis," *Chemical Reviews* 124, no. 10 (2024): 6393–6443.
43. L. Giorno, E. Drioli, and H. Strathmann, "Ion-Exchange Membrane Characterization," in *Encyclopedia of Membranes*, ed. E. Drioli and L. Giorno (Springer Berlin Heidelberg, 2016), 1052–1056.
44. F. Karas, J. Hnat, M. Paidar, J. Schauer, and K. Bouzek, "Determination of the Ion-Exchange Capacity of Anion-Selective Membranes," *International Journal of Hydrogen Energy* 39, no. 10 (2014): 5054–5062.
45. K. Hagesteijn, S. Jiang, and B. Ladewig, "A Review of the Synthesis and Characterization of Anion Exchange Membranes," *Journal of Materials Science* 53, no. 16 (2018): 11131–11150.
46. C. Vogel and J. Meier-Haack, "Preparation of Ion-Exchange Materials and Membranes," *Desalination* 342 (2014): 156–174.
47. M. L. Jordan, T. Kulkarni, D. I. Senadheera, R. Kumar, Y. J. Lin, and C. G. Arges, "Imidazolium-Type Anion Exchange Membranes for Improved Organic Acid Transport and Permselectivity in Electrodialysis," *Journal of the Electrochemical Society* 169, no. 4 (2022): 043511.
48. <https://onlinelibrary.wiley.com/doi/pdf/10.1002/9781119163411.app7>. Accessed on August 28, 2024.
49. I. Vincent, A. Kruger, and D. Bessarabov, "Development of Efficient Membrane Electrode Assembly for Low Cost Hydrogen Production by Anion Exchange Membrane Electrolysis," *International Journal of Hydrogen Energy* 42, no. 16 (2017): 10752–10761.
50. *Fumatech*, Accessed on August 28, 2024 <https://www.fuelcellstore.com/spec-sheets/fumasep-faa-3-50-technical-specifications.pdf>.
51. J. E. Park, S. Y. Kang, S. Oh, et al., "High-Performance Anion-Exchange Membrane Water Electrolysis," *Electrochimica Acta* 295 (2019): 99–106.
52. Aemion, Accessed on August 30, 2024 <https://ionomr.com/wp-content/uploads/2018/12/Ionomr-Hydrogen-Info-Sheet.pdf>.
53. P. Fortin, T. Khoza, X. Cao, S. Y. Martinsen, A. Oyarce Barnett, and S. Holdcroft, "High-Performance Alkaline Water Electrolysis Using Aemion™ Anion Exchange Membranes," *Journal of Power Sources* 451 (2020): 227814.
54. T. Wang, Y. Wang, and W. You, "Dithiol Cross-Linked Polynorbornene-Based Anion-Exchange Membranes With High Hydroxide Conductivity and Alkaline Stability," *Journal of Membrane Science* 685 (2023): 121916.
55. D. Henkensmeier, M. Najibah, C. Harms, J. Žitka, J. Hnat, and K. Bouzek, "Overview: State-of-the Art Commercial Membranes for Anion Exchange Membrane Water Electrolysis," *Journal of Electrochemical Energy Conversion and Storage* 18 (2020): 1–46.
56. C. Liu, Z. Geng, X. Wang, et al., "Development of Advanced Anion Exchange Membrane From the View of the Performance of Water Electrolysis Cell," *Journal of Energy Chemistry* 90 (2024): 348–369.
57. A. W. Tricker, T. Y. Ertugrul, J. K. Lee, et al., "Pathways Toward Efficient and Durable Anion Exchange Membrane Water Electrolyzers Enabled by Electro-Active Porous Transport Layers," *Advanced Energy Materials* 14, no. 9 (2024): 2303629.
58. L. Liu, H. Ma, M. Khan, and B. S. Hsiao, "Recent Advances and Challenges in Anion Exchange Membranes Development/Application for Water Electrolysis: A Review," *Membranes* 14 (2024): 85, <https://doi.org/10.3390/membranes14040085>.

59. Y. Leng, G. Chen, A. J. Mendoza, T. B. Tighe, M. A. Hickner, and C. Wang, "Solid-State Water Electrolysis With an Alkaline Membrane," *Journal of the American Chemical Society* 134, no. 22 (2012): 9054–9057.
60. R. Rossi, R. Taylor, and B. Logan, "Increasing the Electrolyte Salinity to Improve the Performance of Anion Exchange Membrane Water Electrolyzers," *ACS Sustainable Chemistry & Engineering* 11, no. 23 (2023): 8573–8579.
61. H. Ito, N. Miyazaki, S. Sugiyama, et al., "Investigations on Electrode Configurations for Anion Exchange Membrane Electrolysis," *Journal of Applied Electrochemistry* 48 (2018): 305–316.
62. H. Ito, N. Kawaguchi, S. Someya, et al., "Experimental Investigation of Electrolytic Solution for Anion Exchange Membrane Water Electrolysis," *International Journal of Hydrogen Energy* 43, no. 36 (2018): 17030–17039.
63. H. Park, C. Li, and P. Kohl, "Performance of Anion Exchange Membrane Water Electrolysis With High Ionic Strength Electrolyte," *Journal of the Electrochemical Society* 171, no. 2 (2024): 024506.
64. A. Kiessling, J. C. Fornaciari, G. Anderson, et al., "Influence of Supporting Electrolyte on Hydroxide Exchange Membrane Water Electrolysis Performance: Catholyte," *Journal of the Electrochemical Society* 169, no. 2 (2022): 024510.
65. Q. Xu, Z. S. Oener, G. Lindquist et al., "Correction to "Integrated Reference Electrodes in Anion-Exchange-Membrane Electrolyzers: Impact of Stainless-Steel Gas-Diffusion Layers and Internal Mechanical Pressure",," *ACS Energy Letters* 6, no. 6 (2021): 2238–2239.
66. A. Lim, H. Kim, D. Henkensmeier, et al., "A Study on Electrode Fabrication and Operation Variables Affecting the Performance of Anion Exchange Membrane Water Electrolysis," *Journal of Industrial and Engineering Chemistry* 76 (2019): 410–418.
67. A. Capri, I. Gatto, C. Lo Vecchio, S. Trocino, A. Carbone, and V. Baglio, "Anion Exchange Membrane Water Electrolysis Based on Nickel Ferrite Catalysts," *ChemElectroChem* 10, no. 1 (2023): e202201056.
68. A. M. I. Noor Azam, T. Ragunathan, N. N. Zulkefli, et al., "Investigation of Performance of Anion Exchange Membrane (AEM) Electrolysis With Different Operating Conditions," *Polymers* 15 (2023): 1301, <https://doi.org/10.3390/polym15051301>.
69. C. European, et al., *EU Harmonized Protocols for Testing of Low Temperature Water Electrolysis* (Publications Office, 2021). Accessed on September 5, 2024, <https://publications.jrc.ec.europa.eu/repository/handle/JRC122565>.
70. S. Alia, D. Ding, A. McDaniel, F. M. Toma, and H. N. Dinh, "Chalkboard 2-How to Make Clean Hydrogen," *Electrochemical Society Interface* 30, no. 4 (2021): 49.
71. G. Bender, M. Carmo, T. Smolinka, et al., "Initial Approaches in Benchmarking and Round Robin Testing for Proton Exchange Membrane Water Electrolyzers," *International Journal of Hydrogen Energy* 44, no. 18 (2019): 9174–9187.
72. J. A. Wrubel, C. Milleville, E. Klein, J. Zack, A. M. Park, and G. Bender, "Estimating the Energy Requirement for Hydrogen Production in Proton Exchange Membrane Electrolysis Cells Using Rapid Operando Hydrogen Crossover Analysis," *International Journal of Hydrogen Energy* 47, no. 66 (2022): 28244–28253.
73. L. Wang, T. Weissbach, R. Reissner, et al., "High Performance Anion Exchange Membrane Electrolysis Using Plasma-Sprayed, Non-Precious-Metal Electrodes," *ACS Applied Energy Materials* 2, no. 11 (2019): 7903–7912.
74. D. Xu, M. B. Stevens, M. R. Cosby, et al., "Earth-Abundant Oxygen Electrocatalysts for Alkaline Anion-Exchange-Membrane Water Electrolysis: Effects of Catalyst Conductivity and Comparison With Performance in Three-Electrode Cells," *ACS Catalysis* 9, no. 1 (2019): 7–15.
75. A. Loh, X. Li, S. Sluijter, P. Shirvanian, Q. Lai, and Y. Liang, "Design and Scale-Up of Zero-Gap AEM Water Electrolyzers for Hydrogen Production," *Hydrogen* 4 (2023): 257–271, <https://doi.org/10.3390/hydrogen4020018>.
76. J. E. Park, S. Park, M. Kim, et al., "Three-Dimensional Unified Electrode Design Using a NiFeOOH Catalyst for Superior Performance and Durable Anion-Exchange Membrane Water Electrolyzers," *ACS Catalysis* 12, no. 1 (2022): 135–145.
77. R. Wang, M. Ohashi, M. Ishida, and H. Ito, "Water Transport Analysis During Cathode Dry Operation of Anion Exchange Membrane Water Electrolysis," *International Journal of Hydrogen Energy* 47, no. 97 (2022): 40835–40848.
78. H. M. Tee, H. Park, P. N. Shah, J. A. Trindell, J. D. Sugar, and P. A. Kohl, "Self-Adhesive Ionomers for Alkaline Electrolysis: Optimized Hydrogen Evolution Electrode," *Journal of the Electrochemical Society* 169, no. 12 (2022): 124515.
79. N. Ul Hassan, M. J. Zachman, M. Mandal, et al., "Understanding Recoverable vs. Unrecoverable Voltage Losses and Long-Term Degradation Mechanisms in Anion Exchange Membrane Fuel Cells," *ACS Catalysis* 12, no. 13 (2022): 8116–8126.
80. H. Park, P. N. Shah, H. M. Tee, and P. A. Kohl, "Self-Adhesive Ionomers for Alkaline Electrolysis: Optimized Oxygen Evolution Electrode," *Journal of Power Sources* 564 (2023): 232811.
81. Y. Zheng, W. Ma, A. Serban, A. Allushi, and X. Hu, "Anion Exchange Membrane Water Electrolysis at 10 A cm⁻² Over 800 Hours," *Angewandte Chemie International Edition* 64, no. 1 (2025): e202413698.
82. W. Song, K. Peng, W. Xu, et al., "Upscaled Production of an Ultramicroporous Anion-Exchange Membrane Enables Long-Term Operation in Electrochemical Energy Devices," *Nature Communications* 14, no. 1 (2023): 2732.
83. X. Luo, S. Rojas-Carbonell, Y. Yan, and A. Kusoglu, "Structure-Transport Relationships of Poly(Aryl Piperidinium) Anion-Exchange Membranes: Effect of Anions and Hydration," *Journal of Membrane Science* 598 (2020): 117680.